Quantum Sieving

DOI: 10.1002/anie.201307443

A Cryogenically Flexible Covalent Organic Framework for Efficient Hydrogen Isotope Separation by Quantum Sieving**

Hyunchul Oh, Suresh Babu Kalidindi, Youngje Um, Sareeya Bureekaew, Rochus Schmid, Roland A. Fischer, and Michael Hirscher**

Conventional molecular sieves are often utilized in industry for the purification of gas mixtures consisting of different molecular sizes. However, separation of hydrogen isotopes requires special efforts because of their identical size, shape, and thermodynamic properties. Separation of isotope mixtures is only possible with limited techniques, such as cryogenic distillation, thermal diffusion, and the Girdler sulfide process, but these methods have a low separation factor and are excessively time- and energy-intensive.[1] Quantum sieving (QS) of isotopes by confinement in a narrow space has recently been proposed as an attractive alternative[2] and has been tested for various porous materials;[3] however, almost all materials show a low separation factor. The QS effect is pronounced in systems where the difference between pore size and molecular size becomes comparable to the de Broglie wavelength. In this confinement, the zero-point energy of gas molecules overcompensates the interaction potential and thereby produces greater diffusion barriers for lighter isotopes.[2a] Therefore, the aperture size plays a vital role in determining the overall separation.[4]

Covalent organic frameworks (COFs) are microporous organic frameworks and exhibit exceptional high thermal stabilities, low mass densities, and large surface areas.[5] Herein, we report a novel strategy to effectively decrease the aperture size by incorporating pyridine molecules (Py) in the pore walls of COF-1 (C_3H_2BO; Figure 1). This Py@COF-1 has been successfully synthesized and its gas adsorption properties are studied with special focus on separation of hydrogen isotope mixtures by QS.

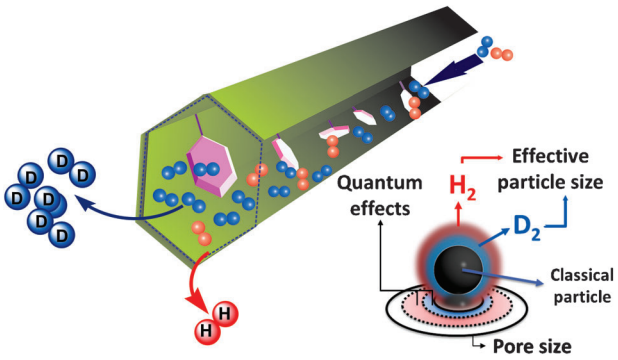

Figure 1. View of the pore channel of COF-1 with dangling pyridine molecules incorporated in the pore walls. The decreased size and the cryogenic flexibility of the aperture are employed for the enhancement of the quantum sieving effect for light isotopes.

Py@COF-1 is synthesized by the Lewis base (Py) assisted condensation of 1,4-benzenediboronic acid (BDBA) (Figure 2a).[5b] Presence of Py drastically lowers the condensation temperature of BDBA from 120 °C to room temperature. The IR (Supporting Information, Figure S1) and ^{11}B and ^{13}C NMR (SI, Figures S2, S3) spectra of this compound are in very good correlation with the respective spectrum of the model compound ($Ph_3B_3O_3$·Py). Thermal gravimetric analysis (SI, Figure S4) of Py@COF-1 shows a weight loss of 29(±2)% around 150 °C, corresponding to loss of one Py molecule per one boroxine ring. This is corroborated by C, H, N analysis data, which is consistent with a molecular formula of $C_3H_2BO{\cdot}1/3\,C_5H_5N$. The SEM data (SI, Figure S5) reveal a plate-like morphology, similar to the parent COF-1. Complete stripping of pyridine from Py@COF-1 gave neat COF-1 (SI, Figures S6, S7). Although, the powder pattern (Figure 2e) of Py@COF-1 contains some broad peaks, the presence of several well-defined peaks indicates an ordered structure. Importantly, the peak at $2\theta = 26.8°$ corresponds to a typical π–π stacking distance, similar to the parent COF-1, indicating a close packed structure of Py@COF-1.

Recently, theoretical investigations[6] proposed a hypothetical structure for Py@COF-1 based on three different stacking patterns, which were optimized by periodic density functional theory (DFT) calculations. In all cases, a large layer separation above 7.5 Å was found and the pillaring of COF-1 by Py was suggested as a method to increase porosity. Our experimental data clearly contradicts this pillaring and rules

[*] H. Oh,[+] Dr. M. Hirscher
Max Planck Institute for Intelligent Systems
Heisenbergstrasse 3, 70569 Stuttgart (Germany)
E-mail: hirscher@is.mpg.de
Dr. S. B. Kalidindi,[+] Dr. S. Bureekaew, Dr. R. Schmid, Prof. Dr. R. A. Fischer
Inorganic Chemistry II—Organometallics & Materials
Faculty of Chemistry and Biochemistry, Ruhr University Bochum
44780 Bochum (Germany)
E-mail: roland.fischer@rub.de
Y. Um
Max Planck Institute for Solid States Research
Heisenbergstrasse 1, 70569 Stuttgart (Germany)
[+] These authors contributed equally to this work.

[**] H.O. is grateful for a scholarship from the International Max Planck Research School for Advanced Materials (IMPRS-AM). Partial funding by the German Research Foundation (DFG) within the priority program SSP 1362 is gratefully acknowledged by authors. S.B.K. thanks AvH foundation for a fellowship. We thank Abhishek Kanitkar for his help with the initial experiments.
Supporting information for this article is available on the WWW under http://dx.doi.org/10.1002/anie.201307443.

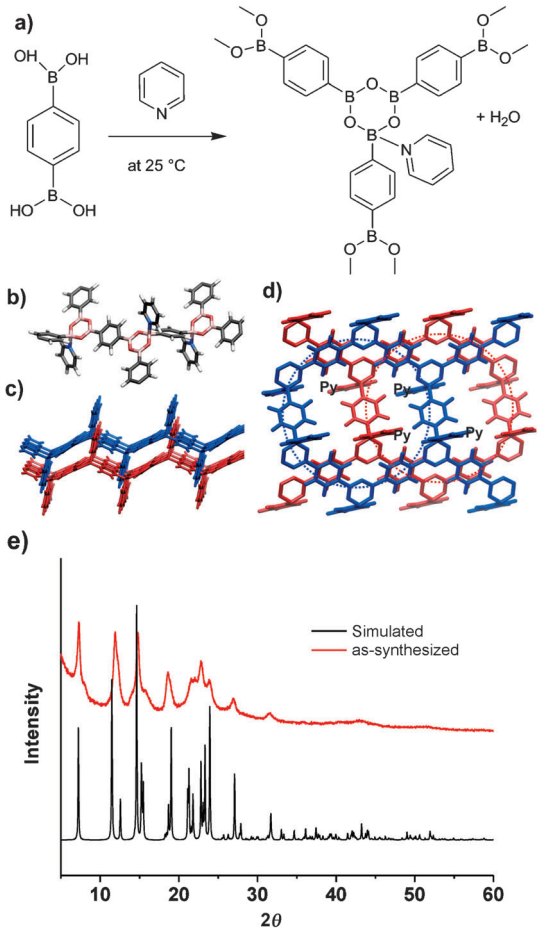

Figure 2. a) Synthesis of Py@COF-1 from 1,4-benzenediboronic acid by the Lewis base assisted pathway. b) Bent structure of a single layer; c) close packing of two layers. d) Top view of the ABAB stacking pattern of the layers (blue top layer and red bottom layer). e) Comparison of simulated and experimental powder XRD patterns of Py@COF-1.

out these proposed structures for Py@COF-1. For a more thorough theoretical structure prediction, we have used our recently developed reverse topological approach (RTA) in combination with the genetic algorithm global optimization strategy[7] (see the Supporting Information). With this novel approach, we could identify the energetically most preferred stacking pattern. By breaking the symmetry in the 2D layer, the Py adducts are distributed in a way that allows a dense packing of two layers (Figure 2c). By a ABAB stacking pattern (see Figure 2d) the Py of one layer occupies the hexagonal pore space of the layer above/below, which will effectively decrease the aperture size of the COF-1 channels that is relevant for gas penetration. The dense packing allows maximum dispersive interactions between the system of adjacent layers and results in an energetic minimum.

Note that the more open hypothetical structures suggested in Ref. [6] (reoptimized on our level of theory[8]) are 17 kcal mol^{-1} per formula unit ($(B_3O_3)_2(Ph)_3(Py)_2$) higher in energy compared to the global minimum. The simulated PXRD of our final structure model compares very well with the experimental data as shown in Figure 2e. The experimental peaks are broadened, which is probably also due to defects in the Py position, which could lead to stacking faults and a certain disorder. Overall, the theoretically predicted structure is a very good, but somewhat idealized atomistic, structure model for Py@COF-1.

Gas adsorption measurements performed on this highly dense structure possessing a decreased aperture size show that neither N_2 at 77 K nor H_2 at 19.5 K can penetrate Py@COF-1, whereas the parent COF-1 is fully accessible for these molecules. An analysis of the isotherms results in BET areas of 20.5 $m^2 g^{-1}$ and 48 $m^2 g^{-1}$ applying N_2 and H_2, respectively (SI, Figure S8), confirming the blocked apertures as evident from the dense structure (Figure 2d).

This dense structure of Py@COF-1 exhibits unique sorption behavior at low temperatures (19.5–70 K) as shown in Figure 3 (see also the SI, Figure S12). Gas uptake starts at

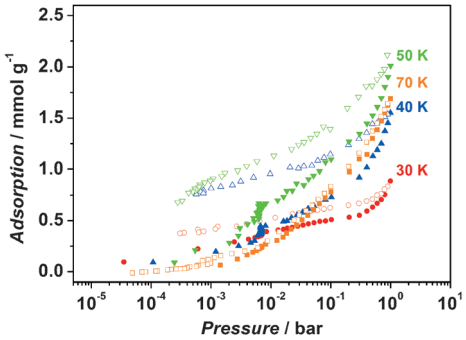

Figure 3. Hydrogen ad/desorption isotherms of Py@COF-1: closed symbol is adsorption and open symbol is desorption at various temperature at 30 K (red circle), 40 K (blue triangle), 50 K (green inverse triangle), and 70 K (square orange). See the Supporting Information, Figure S13 for additional 19.5 K and 60 K isotherms.

30 K, exhibiting a hysteresis (Figure 3). The observed hysteresis becomes stronger up to 40 K, then weaker above 50 K. The maximum hydrogen uptake is found at 50 K. These hystereses indicate the slow diffusion kinetics between 30 and 70 K (Figure 3; SI, Figure S12). In particular, a varying degree of hysteresis indicates changes in the effective aperture size experienced by the adsorbate, implying a flexible aperture and gating effects. This higher accessibility of hydrogen is also evident from the increase in surface area from 20.5 $m^2 g^{-1}$ at 19.5 K to 250 $m^2 g^{-1}$ at 77 K (derived from the linear relationship between excess H_2 uptake and surface area; SI, Figure S14). It should be noted that flexible frameworks reported in literature are typically accompanied by a volume change of the framework (for example, structural deformation of MIL-53), whereas the flexibility described in here implies only a kinetic effect caused by the pyridine molecules in the pore (no structural deformation).

A close comparison of the Raman spectra between Py@COF-1 and pristine COF-1 also supports the cryogenically flexible nature caused by Py molecules (SI, Figures S15, S16). We carefully analyzed low-energy Raman active phonon modes that cannot originate from the free Py or pristine COF-1. The 50 cm^{-1} phonon mode hardens with decreasing temperature down to 30 K, and then softens down

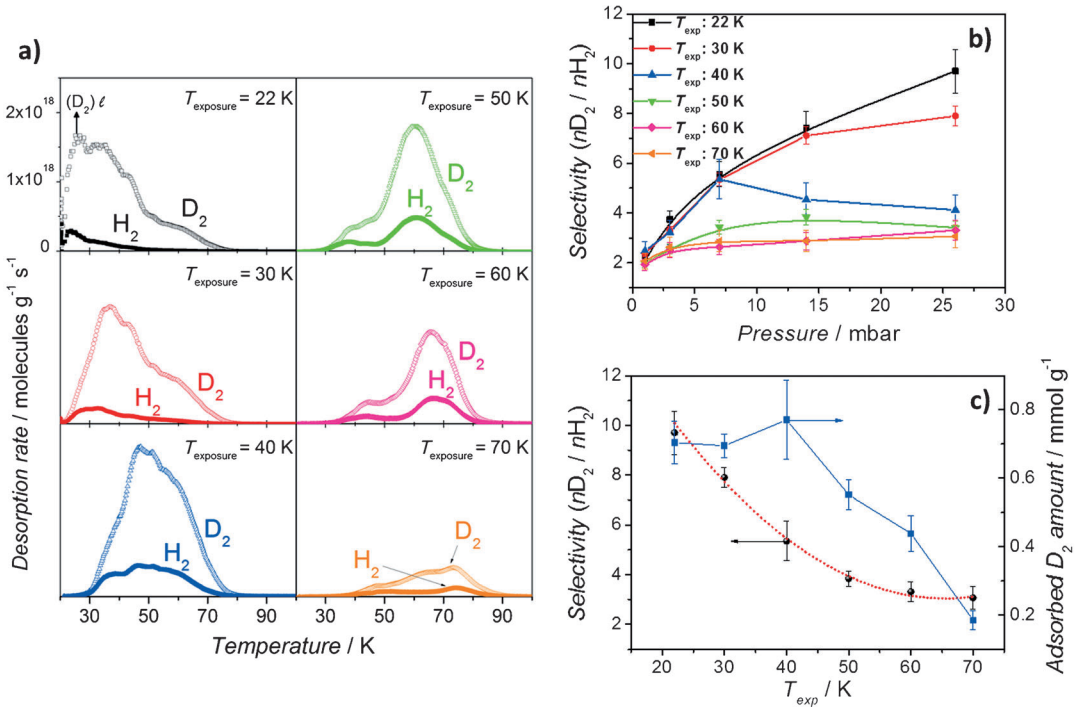

Figure 4. a) H_2 and D_2 TDS of 26 mbar (1:1 H_2/D_2 mixture) loading on Py@COF-1 with heating rate 0.1 K s^{-1}; loading temperature (T_{exp}) at 22 K (black square), 30 K (red circle) 40 K (blue triangle), 50 K (green triangle), 60 K (pink diamond), and 70 K (orange triangle). b) Equimolar mixture selectivity as a function of loading pressure for different T_{exp}. c) T_{exp} dependence of the maximum selectivity and corresponding adsorbed D_2 amount.

to base temperature. The observed phonon softening implies a redistribution of the electronic state at below 30 K, which predominantly contributes the phonon self-energy, suggesting a re-orientation of the Py molecule with respect to the backbone of COF-1. Owing to this unique phenomenon, the hysteresis in isotherms starts to be observed at 30 K until the reversible isotherm appears at 70 K owing to the fully open aperture for hydrogen. Note that identical phenomena are also observed in case of D_2 pure gas adsorption; however, the adsorbed amount is higher than for H_2 indicating quantum effects (SI, Figure S13).

As cryogenic flexibility produces a kinetic hindrance at the aperture, we anticipate that this kind of materials could be an excellent candidate for hydrogen isotope separation. To exploit the cryogenic flexibility of Py@COF-1 for QS, the D_2/H_2 molar ratio based on the pure gas isotherms are assessed (SI, Figure S17b), and compared it with pristine COF-1 (SI, Figure S17a).[4] For the pristine COF-1, the highest molar ratio is only observed at near-zero coverage pressure and decays rapidly for higher pressures. In contrast, the molar ratio for Py@COF-1 shows a maximum at about one order of magnitude higher pressures for temperatures between 19.5 K and 40 K.

Motivated by this enhanced molar ratio at higher pressures for pure gas isotherms, the selectivity was directly investigated for a H_2/D_2 isotope mixture by employing a home-built thermal desorption spectroscopy (TDS) apparatus,[3d,9] which is calibrated for H_2 and D_2. After cooling in high vacuum to a given exposure temperature, T_{exp}, of 22 to 70 K, the sample is exposed to an equimolar H_2/D_2 mixture for different loading pressures of 1 to 26 mbar. After 0.5 h exposure, the chamber is evacuated, the sample cooled rapidly to 20 K, and the TDS run started (heating rate 0.1 K s^{-1}), with simultaneous recording of the H_2 and D_2 signal (for more details, see the SI, Figure S18). Figure 4a shows H_2 and D_2 TDS of Py@COF-1 for 26 mbar loading pressure in the temperature range between 20 and 100 K; above 100 K no significant desorption of hydrogen isotopes is occurring. The H_2 and D_2 TDS spectra (SI, Figures S19, S20, respectively) show all of the loading pressures and exposure temperatures. For all of the measurements, the area under the desorption curve, which is directly proportional to the amount of molecules, is significantly higher for D_2 than for H_2, owing to quantum effects occurring during the adsorption process. Furthermore, depending on the exposure temperature, the spectra vary in shape, magnitude, and desorption temperature. For the lowest T_{exp} (22 K), the D_2 spectrum shows the highest desorption rate at 25 K, which can be assigned to liquid deuterium or D_2 weakly adsorbed in multilayers.[10] For higher exposure temperatures, the spectrum is shifted to higher desorption temperatures. The missing low temperature part of the spectrum is simply caused by desorption of weakly adsorbed molecules already during the evacuation at T_{exp}, whereas an increase of desorption temperature with T_{exp} is unusual for porous materials. In accordance with our observations of the pure gas isotherms, this can be attributed to the flexible nature of the framework, which eventually gives different effective apertures at each T_{exp} (pore-opening phenomenon) and thereby increasing accessibility for gas molecules. Additional evidence can be found in the H_2 and D_2

spectra for different loading pressure and T_{exp} (SI, Figures S19, S20). The amount of desorbed D_2 increases with rising pressure up to $T_{exp} = 40$ K. In contrast, the H_2 uptake decreases, with rising pressure at $T_{exp} = 22$ and 30 K and at $T_{exp} = 40$ K the uptake shows a minimum at 7 mbar. This observation suggests that until 40 K and 7 mbar the flexible aperture of Py@COF-1 possesses the optimum size for preferential D_2 adsorption by QS.

From TDS, the direct mixture selectivity can be determined from the ratio of desorbed amount of D_2 over H_2 (S_{D_2/H_2}). The selectivity for a 1:1 D_2/H_2 mixture (Figure 4b) is significantly greater than those of molar ratio from pure gas isotherms (SI, Figure S17). This is because: 1) the heavier D_2 favors adsorption on the surface owing to the quantum isotope effect;[11] and 2) D_2 diffuses faster compare to the H_2 through the aperture into the nanoporous material at low temperatures.[2a] Owing to these two effects and cryogenic flexibility, S_{D_2/H_2} at $T_{exp} < 30$ K increases with pressure and reaches to $S_{D_2/H_2} S_{D_2/H_2} = 9.7 \pm 0.9$ at 26 mbar. The S_{D_2/H_2} value for all exposure temperatures examined and pressures of 1 to 26 mbar are summarized in the SI, Table S1. The observed high selectivity at $T_{exp} < 30$ K can be ascribed to combined effect of QS and liquefaction of D_2. It is noteworthy that the observed selectivity is far more superior compared to commercial cryogenic distillation process ($S_{D_2/H_2} \approx 1.5$ at 24 K[1]). Eventually S_{D_2/H_2} drops down to 3.1 ± 0.5 at 70 K, but its selectivity and amount of adsorbed D_2 (Figure 4c) are still comparable to the very recently reported highest experimental value of 3.05 and 0.2 mmol g^{-1} at 77 K, respectively.[3c] Furthermore, the relatively high selectivity combined with large D_2 uptake at $T_{exp} = 40$ K (Figure 4c) indicates the optimum conditions of the cryogenically flexible aperture for QS. These conditions may be very interesting for industrial applications considering the obtained amount of D_2 and the lower energy consumption compared to cryogenic distillation at 22 K.

In summary, we have successfully synthesized Py@COF-1 using a Lewis base approach, and its highly dense packing structure has been experimentally characterized and theoretically established using a novel combination of reverse topological approach and the genetic algorithm global optimization strategy. Installation of pyridine molecules on the pore walls of COF-1 effectively decreased aperture size and pore volume. Already at low temperatures (> 30 K) the system shows cryogenic flexibility, which enables highly selective quantum sieving of D_2 from a 1:1 H_2/D_2 isotope mixture. It is expected that this work will initiate further research on aperture engineering of COFs, and lead to intelligently designed porous materials which can be applied for various isotope separations, including ^{3}He/^{4}He.

Received: August 23, 2013
Published online: November 11, 2013

Keywords: covalent organic frameworks · gas adsorption · hydrogen isotopes · isotope separation · quantum sieving

[1] K. Rae H, *Separation of Hydrogen Isotopes*, *Vol. 68*, American Chemical Society, **1978**, pp. 1–26.
[2] a) J. J. M. Beenakker, V. D. Borman, S. Y. Krylov, *Chem. Phys. Lett.* **1995**, *232*, 379–382; b) J. Cai, Y. Xing, X. Zhao, *RSC Adv.* **2012**, *2*, 8579–8586.
[3] a) D. Noguchi, H. Tanaka, A. Kondo, H. Kajiro, H. Noguchi, T. Ohba, H. Kanoh, K. Kaneko, *J. Am. Chem. Soc.* **2008**, *130*, 6367–6372; b) H. Kagita, T. Ohba, T. Fujimori, H. Tanaka, K. Hata, S.-i. Taira, H. Kanoh, D. Minami, Y. Hattori, T. Itoh, H. Masu, M. Endo, K. Kaneko, *J. Phys. Chem. C* **2012**, *116*, 20918–20922; c) S. Niimura, T. Fujimori, D. Minami, Y. Hattori, L. Abrams, D. Corbin, K. Hata, K. Kaneko, *J. Am. Chem. Soc.* **2012**, *134*, 18483–18486; d) J. Teufel, H. Oh, M. Hirscher, M. Wahiduzzaman, L. Zhechkov, A. Kuc, T. Heine, D. Denysenko, D. Volkmer, *Adv. Mater.* **2013**, *25*, 635–639.
[4] H. Oh, K. S. Park, S. B. Kalidindi, R. A. Fischer, M. Hirscher, *J. Mater. Chem. A* **2013**, *1*, 3244–3248.
[5] a) O. M. Yaghi, H. M. El-Kaderi, J. R. Hunt, J. L. Mendoza-Cortes, A. P. Cote, R. E. Taylor, M. O'Keeffe, *Science* **2007**, *316*, 268–272; b) S. B. Kalidindi, C. Wiktor, A. Ramakrishnan, J. Weßing, A. Schneemann, G. V. Tendeloo, R. A. Fischer, *Chem. Commun.* **2013**, *49*, 463–465.
[6] D. Kim, D. H. Jung, K.-H. Kim, H. Guk, S. S. Han, K. Choi, S.-H. Choi, *J. Phys. Chem. C* **2011**, *115*, 1479–1484.
[7] S. Bureekaew, R. Schmid, *CrystEngComm* **2013**, *15*, 1551–1562.
[8] S. Bureekaew, S. Amirjalayer, M. Tafipolsky, C. Spickermann, T. K. Roy, R. Schmid, *Phys. Status Solidi B* **2013**, *250*, 1128–1141.
[9] B. Panella, M. Hirscher, B. Ludescher, *Microporous Mesoporous Mater.* **2007**, *103*, 230–234.
[10] B. Panella, K. Hönes, U. Müller, N. Trukhan, M. Schubert, H. Pütter, M. Hirscher, *Angew. Chem.* **2008**, *120*, 2169–2173; *Angew. Chem. Int. Ed.* **2008**, *47*, 2138–2142.
[11] B. Chen, X. Zhao, A. Putkham, K. Hong, E. B. Lobkovsky, E. J. Hurtado, A. J. Fletcher, K. M. Thomas, *J. Am. Chem. Soc.* **2008**, *130*, 6411–6423.

